Available online at www.sciencedirect.com
SCIENCE DIRECT®
ELSEVIER
International Journal of Heat and Mass Transfer 47 (2004) 969–976
International Journal of HEAT and MASS TRANSFER
www.elsevier.com/locate/ijhmt

Mixed convection boundary layer flow over a thin vertical cylinder with localized injection/suction and cooling/heating

M. Kumari *, G. Nath

Department of Mathematics, Indian Institute of Science, Bangalore 560012, India

Received 7 February 2003; received in revised form 8 August 2003

Abstract

The effects of localized cooling/heating and injection/suction on the mixed convection flow on a thin vertical cylinder have been studied. The localized cooling/heating and (or) injection/suction introduce a finite discontinuity in the mathematical formulation of the problem which increases its complexity. In order to overcome this difficulty, a non-uniform distribution of wall temperature (heat flux) and surface mass transfer is considered at certain sections of the cylinder. The nonlinear coupled parabolic partial differential equations governing the mixed convection flow under boundary layer approximations have been solved numerically by using an implicit finite-difference scheme. The effects of the localized cooling/heating and (or) injection/suction on the heat transfer are found to be significant, but the effects of cooling/heating on the skin friction are comparatively small. The positive buoyancy force which assists the flow and the curvature parameter increase the skin friction and heat transfer.

1. Introduction

The combined forced and free convection flow (mixed convection flow) is encountered in several industrial and technical applications such as nuclear reactors cooled during emergency shutdown, electronics devices cooled by fans, heat exchangers placed in a low-velocity environment, solar central receivers exposed to wind currents, etc.

Flow over cylinders is considered to be two-dimensional if the body radius is large compared to the boundary layer thickness. For a thin or slender cylinder, the radius of the cylinder may be of the same order as the boundary layer thickness. Therefore, the flow may be considered as axisymmetric instead of two-dimensional. In this case, the governing equations contain the transverse curvature term which influences both the velocity and temperature fields. The effect of the transverse curvature is important in certain applications such as wire or fibre drawing where accurate prediction of flow and heat transfer is required and thick boundary layer can exist on slender or near slender bodies.

There are only a few papers in the literature that deal with mixed convection flow over vertical cylinders. Chen and Mucoglu [1] were the first to study such a problem for a uniform wall temperature case. Subsequently, Mucoglu and Chen [2] considered the same problem for the uniform surface heat flux case. In both cases, solutions of the governing boundary layer equations were obtained by the local nonsimilarity method [3,4]. Bu and Cebeci [5] and Wang and Kleinstrever [6] considered the same problem for the case of uniform wall temperature and solved the governing boundary layer equations by using a finite-difference scheme [7] based on the central difference scheme (Keller box method). In the above studies, the effect of buoyancy force on the forced convection flow was considered. Lee et al. [8,9] investigated the same flow configuration under uniform surface temperature and heat flux conditions for the entire range of mixed convection, from pure forced convection at one end to pure free convection at the other end. The

* Corresponding author. Tel.: +91-80-2933214/2932265; fax: +91-80-3600146.
E-mail address: mkumari@math.iisc.ernet.in (M. Kumari).

0017-9310/$ - see front matter © 2003 Elsevier Ltd. All rights reserved.
doi:10.1016/j.ijheatmasstransfer.2003.08.014

Nomenclature

C_{fx}	local skin friction coefficient
f	reduced stream function
f' $(=F)$	dimensionless velocity
g	local gravitational acceleration ($\mathrm{m\,s^{-2}}$)
Gr_x, Gr_x^*	local Grashof numbers for the VWT and VHF cases, respectively
Gr_R, Gr_R^*	Grashof numbers with respect to R for the VWT and VHF cases, respectively
H	dimensionless dependent variable
k	thermal conductivity of the fluid ($\mathrm{W\,m^{-1}\,K}$)
m	dimensionless mass transfer
Nu_x	local Nusselt number
Pr	Prandtl number
q_w	surface heat flux ($\mathrm{W\,m^{-2}}$)
q_0	constant heat flux at the surface ($\mathrm{W\,m^{-2}}$)
r	radial coordinate (m)
R	radius of the cylinder (m)
Re_x, Re_R	Reynolds numbers defined with respect to x and R, respectively
T	temperature (K)
T_0	constant temperature (K)
u, v	axial and radial velocity components ($\mathrm{m\,s^{-1}}$)
x	axial coordinate (m)

Greek symbols

α	thermal diffusivity ($\mathrm{m^2\,s^{-1}}$)
β	volumetric coefficient of thermal expansion ($\mathrm{K^{-1}}$)
η, ξ, η^*, ξ^*	transformed coordinates
ξ_1	dimensionless curvature
μ	coefficient of viscosity ($\mathrm{kg\,m^{-2}\,s^{-1}}$)
θ	dimensionless temperature
λ, λ^*	buoyancy parameters defined in Eqs. (5) and (12)
ν	kinematic viscosity ($\mathrm{m^2\,s^{-1}}$)
ρ	density ($\mathrm{kg\,m^{-3}}$)
ψ	stream function ($\mathrm{m^3\,s^{-1}}$)
ϵ_1, ϵ_2, ϵ_3	dimensionless constants

Subscripts

r, x	denotes derivatives with respect to r and x, respectively
w, ∞	denote conditions at the wall and in the free stream, respectively

Superscript

$'$	prime denotes derivative with respect to η

governing boundary layer equations were solved by a stable finite-difference method [10] in conjunction with the cubic spline interpolation scheme [11] to overcome the difficulties that arise from the stiffness of the equations. Na and Pop [12] have studied the flow and heat transfer characteristics on the longitudinal cylinder which moves parallel or reversely to a free stream and solved the governing equations by an implicit finite-difference scheme. Takhar et al. [13] have considered the mixed convection flow over a vertical thin cylinder due to the combined effect of the thermal and mass diffusion. Both uniform wall temperature and uniform wall heat flux conditions were included in the analysis. The governing boundary layer equations were solved by using an implicit finite-difference scheme. In mixed convection flows, the positive buoyancy force and the transverse curvature tend to increase the heat transfer as well as the skin friction. However, it is possible to reduce the skin friction and heat transfer by localized cooling of the surface. It is more practical as well as economic to cool a portion of the surface instead of the entire surface. Similarly, injection or suction can be applied only in a certain portion of the surface rather than on the entire surface. If the entire surface is made permeable, the body will become structurally weak.

In this paper, we consider the effects of cooling/heating and (or) injection/suction at certain sections of the body surface on the steady laminar mixed convection flow over a vertical thin cylinder. It may be remarked that the increase or reduction of wall temperature (heat flux) or mass transfer (injection/suction) in a certain section of the surface introduces a discontinuity at the leading and trailing edges of the slot. This causes certain difficulties in the numerical solution of the governing equations. In order to overcome this difficulty, we have chosen a function representing the distribution of the wall temperature (heat flux) or mass transfer in the slot which varies slowly with the streamwise distance and is continuous in the slot (including the leading and trailing edges of the slot). Both variable wall temperature (VWT) and variable wall heat flux (VHF) conditions have been considered. The coupled nonlinear parabolic partial differential equations governing the mixed convection flow have been solved numerically by using an implicit finite-difference scheme similar to that of Blottner [14]. The results in the absence of wall cooling/heating and injection/suction have been compared with those of Chen and Mucoglu [1] and Mucoglu and Chen [2]. This investigation may be useful in the cooling of nuclear reactors during emergency shutdown, where a part of the surface can be cooled by injecting a coolant. The reactor can also be cooled by removing the heat source through a certain portion of the surface.

2. Analysis

Let us consider a thin vertical circular cylinder of radius R maintained at temperature T_w or at heat flux q_w. Let u_∞ and T_∞ be the velocity and temperature in the free stream. The radial coordinate r is measured from the axis of the cylinder and the axial coordinate x is measured vertically upwards such that $x = 0$ corresponds to the leading edge, where the boundary layer thickness is zero. Fig. 1 shows the physical model and coordinate system. The fluid properties are assumed to be constant except the density changes which give rise to the buoyancy forces. The surface of the cylinder is maintained at a constant temperature T_0 except in certain portions of the cylinder $[x_i, x_j]$ where it varies slowly with the streamwise distance x. There is no mass transfer (suction/injection) on the surface except in the interval $[x_i, x_j]$ where it varies slowly with the distance x. The viscous dissipation has been neglected in the energy equation. It is assumed that the injected gas possesses the same physical properties as the boundary layer gas and has a static temperature equal to the wall temperature. Under the above assumptions, the equations of continuity, momentum and energy under boundary layer approximations governing the mixed convection flow over a thin vertical cylinder can be expressed as [1,2,8,9]

$$(ru)_x + (rv)_r = 0, \tag{1}$$

$$uu_x + vu_r = (\nu/r)(ru)_r + g\beta(T - T_\infty), \tag{2}$$

$$uT_x + vT_r = (\alpha/r)(rT_r)_r. \tag{3}$$

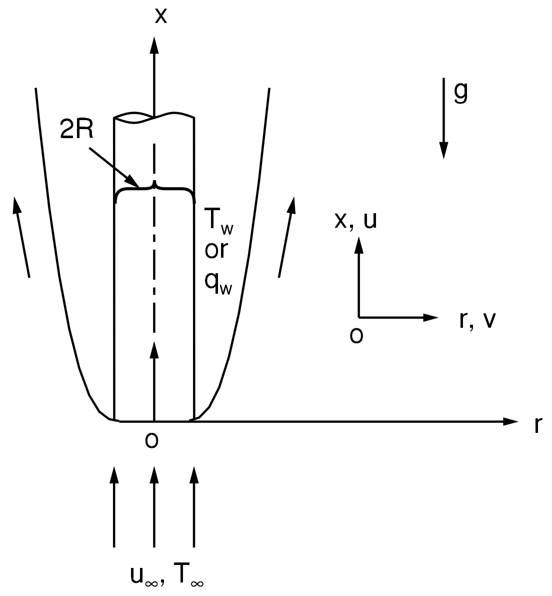

Fig. 1. Physical model and coordinate system.

The boundary conditions for both VWT and VHF conditions are the no-slip conditions at the wall and the free stream conditions far away from the surface and these conditions are given by

$$\begin{aligned}
&u(R,x) = 0, \quad u(\infty,x) = u_\infty, \quad T(\infty,x) = T_\infty,\\
&u(r,0) = u_\infty, \quad T(r,0) = T_\infty, \qquad r > R,\\
&v(R,x) = v_w(x) \quad \text{for } x_i \leqslant x \leqslant x_j,\\
&v(R,x) = 0 \quad \text{for } 0 \leqslant x \leqslant x_i,\ x \geqslant x_j,\\
&\left.\begin{aligned} &T(R,x) = T_w(x) \quad \text{for } x_i \leqslant x \leqslant x_j,\\ &T(R,x) = T_0 \qquad \text{for } 0 \leqslant x \leqslant x_i,\ x \geqslant x_j, \end{aligned}\right\}\\
&\quad \text{(VWT case)}\\
&\left.\begin{aligned} &\partial T(R,x)/\partial r = -q_w(x)/k \quad \text{for } x_i \leqslant x \leqslant x_j,\\ &\partial T(R,x)/\partial r = -q_0/k \qquad \text{for } 0 \leqslant x \leqslant x_i,\ x \geqslant x_j, \end{aligned}\right\}\\
&\quad \text{(VHF case)}
\end{aligned} \tag{4}$$

Here r and x are distances along the radial and axial directions, respectively, u and v are the velocity components along x and r directions, respectively, T is the temperature, g is the magnitude of the acceleration due to gravity, β is the volumetric coefficient of thermal expansion, α is the thermal diffusivity, ν is the kinematic viscosity, q_w is the local surface heat transfer rate per unit mass, R is the radius of the cylinder, k is the thermal conductivity, ρ is the density, T_0 and q_0 are the constant wall temperature and constant wall heat flux, respectively, the subscripts r and x denote derivatives with respect to r and x, respectively, and the subscripts w and ∞ denote conditions at the wall and in the free stream, respectively.

It is convenient to reduce the number of equations from three to two as well as to transform them to dimensionless form. This can be done by applying the following transformations:

$$\begin{aligned}
&\xi = x/R, \quad \eta = (2xR)^{-1}(r^2 - R^2)(Re_x)^{1/2},\\
&Re_x = u_\infty x/\nu, \quad Pr = \nu/\alpha,\\
&u = r^{-1}\partial\psi/\partial r, \quad v = -r^{-1}\partial\psi/\partial x,\\
&Gr_x = g\beta(T_0 - T_\infty)x^3/\nu^2,\\
&\psi(r,x) = Ru_\infty x(Re_x)^{-1/2} f(\xi,\eta) - \int_0^x r v_w \,\mathrm{d}x,\\
&T(r,x) - T_\infty = (T_0 - T_\infty)\theta(\xi,\eta),\\
&Re_R = u_\infty R/\nu, \quad Re_x = \xi Re_R,\\
&\xi_1 = 2\xi^{1/2}(Re_R)^{-1/2}, \quad \lambda = Gr_R/Re_R^2,\\
&Gr_R = g\beta(T_0 - T_\infty)R^3/\nu^2,\\
&m = (v_w/u_\infty)Re_R^{1/2},\\
&(v_w/u_\infty)Re_R^{1/2} = \epsilon_1(\xi - \xi_i)(\xi_j - \xi)(\xi_j - \xi_i)^{-2}\\
&\quad \text{for } \xi_i \leqslant \xi \leqslant \xi_j,\\
&v_w/u_\infty = 0 \quad \text{for } 0 \leqslant \xi \leqslant \xi_i,\ \xi \geqslant \xi_j.
\end{aligned} \tag{5}$$

to Eqs. (1)–(3) and we find that Eq. (1) is identically satisfied and Eqs. (2) and (3) for the VWT case reduce to

$$[(1+\xi_1\eta)f'']' + 2^{-1}ff'' - m(1+\xi_1\eta)^{1/2}\xi^{1/2}f'' + \lambda\xi\theta = \xi(f'\partial f'/\partial\xi - f''\partial f/\partial\xi), \tag{6}$$

$$Pr^{-1}[(1+\xi_1\eta)\theta']' + 2^{-1}f\theta' - m(1+\xi_1\eta)^{1/2}\xi^{1/2}\theta' = \xi(f'\partial\theta'/\partial\xi - \theta'\partial f/\partial\xi). \tag{7}$$

The boundary conditions (4) for the VWT case can be re-written as

$$\begin{aligned} &f(\xi,0) = f'(\xi,0) = 0, \quad f'(\xi,\infty) = 1, \quad \theta(\xi,\infty) = 0,\\ &\theta(\xi,0) = \epsilon_2(\xi-\xi_i)(\xi_j-\xi)/(\xi_j-\xi_i)^2 \quad \text{for } \xi_i \leqslant \xi \leqslant \xi_j,\\ &\theta(\xi,0) = 0 \quad \text{for } 0 \leqslant \xi \leqslant \xi_i,\ \ \xi \geqslant \xi_j. \end{aligned} \tag{8}$$

For VHF case, the equations corresponding to (6) and (7) can be expressed as

$$[(1+\xi_1\eta)f'']' + 2^{-1}ff'' - m(1+\xi_1\eta)^{1/2}\xi^{1/2}f'' + \lambda^*\xi^{3/2}\theta = \xi(f'\partial f'\partial\xi - f''\partial f/\partial\xi), \tag{9}$$

$$Pr^{-1}[(1+\xi_1\eta)\theta']' + 2^{-1}(f\theta' - f'\theta) - m(1+\xi_1\eta)^{1/2}\xi^{1/2}\theta' = \xi(f'\partial\theta/\partial\xi - \theta'\partial f/\partial\xi). \tag{10}$$

The boundary conditions for this case are

$$\begin{aligned} &f(\xi,0) = f'(\xi,0) = 0,\ \ f'(\xi,\infty) = 1,\ \ \theta(\xi,\infty) = 0,\\ &\theta'(\xi,0) = -1 - \epsilon_3(\xi-\xi_i)(\xi_j-\xi)(\xi_j-\xi_i)^{-2}\\ &\quad \text{for } \xi_i \leqslant \xi \leqslant \xi_j,\\ &\theta'(\xi,0) = -1 \ \ \text{for } 0 \leqslant \xi \leqslant \xi_i,\ \xi \geqslant \xi_j, \end{aligned} \tag{11}$$

where

$$\begin{aligned} &T(r,x) - T_\infty = (q_0/k)x(r/R)^{-1}Re_x^{-1/2}\theta(\xi,\eta),\\ &Gr_R^* = g\beta q_0 R^4/(kv^2), \quad \lambda^* = Gr_R^*/Re_R^{5/2},\\ &q_w/q_0 = -1 - \epsilon_3(\xi-\xi_i)(\xi_j-\xi)(\xi_j-\xi_i)^{-2}\\ &\quad \text{for } \xi_i \leqslant \xi \leqslant \xi_j,\\ &q_w/q_0 = -1 \quad \text{for } 0 \leqslant \xi \leqslant \xi_i,\ \ \xi \geqslant \xi_j. \end{aligned} \tag{12}$$

Here ξ and η are transformed coordinates, ψ and f are the dimensional and dimensionless stream functions, respectively, f' is the dimensionless velocity, ξ_1 is the curvature parameter, θ is the dimensionless temperature, Re_R and Re_x are the Reynolds numbers with respect to R and x, respectively, λ and λ^* are the buoyancy parameters for VWT and VHF cases, respectively, Gr_R and Gr_R^* are the Grashof numbers for the VWT and VHF cases, respectively, m denotes the mass transfer distribution, Pr is the Prandtl number, and prime denotes derivative with respect to η.

The local skin friction coefficient C_{fx} and the local heat transfer coefficient in terms of the local Nusselt number Nu_x can be expressed as

$$\begin{aligned} &C_{fx} = \mu(\partial u/\partial r)_{r=R}/\rho u_\infty^2 = Re_x^{-1/2}f''(\xi,0),\\ &Nu_x = -x(\partial T/\partial r)_{r=R}/(T_0 - T_\infty) = -Re_x^{1/2}\theta'(\xi,0)\\ &\quad \text{(VWT case)},\\ &Nu_x = Re_x^{1/2}/\theta(\xi,0) \quad \text{(VHF case)}, \end{aligned} \tag{13}$$

where μ is the coefficient of viscosity.

It may be noted that Eqs. (6)–(11) in the absence of cooling/heating of the wall and injection/suction ($\epsilon_1 = \epsilon_2 = \epsilon_3 = m = 0$) are the same as those of Chen and Mucoglu [1] and Mucoglu and Chen [2] if we apply the following transformations:

$$\begin{aligned} &\eta = 2\eta^*, \quad \xi = 4^{-1}Re_x^{1/2}\xi^*, \quad f(\xi,\eta) = f^*(\xi^*,\eta^*),\\ &\theta(\xi,\eta) = \theta^*(\xi^*,\eta^*), \end{aligned} \tag{14}$$

and replace $\lambda\xi$ and $\lambda^*\xi^{3/2}$ in Eqs. (6) and (9) by Ω and Ω^*, respectively.

3. Numerical method

The nonlinear coupled parabolic partial differential equations (6) and (7) under boundary conditions (8) and Eqs. (9) and (10) under conditions (11) have been solved numerically by using an implicit, iterative tridiagonal finite-difference method similar to that discussed by Blottner [14]. All the first-order derivatives with respect to ξ are replaced by two-point backward difference formulae of the form

$$\partial H/\partial\xi = (H_{i,j} - H_{i-1,j})/\Delta\xi, \tag{15}$$

where H is any dependent variable and i and j are the node locations along ξ and η directions, respectively. First the third-order partial differential equations (6) and (9) are converted into second-order by substituting $f' = F$. Then these second-order equations are discretized by using three-point central difference formulae while all the first-order differential equations are discretized by applying the trapezoidal rule. The function f is calculated from $f = \int_0^\eta F\,d\eta$. The nonlinear terms are evaluated at the previous iteration. At each line of constant ξ, a system of algebraic equations is obtained. These algebraic equations are solved iteratively by using the Thomas algorithm (see Blottner [14]). The same process is repeated for the next ξ value and the equations are solved line by line until the desired ξ value is reached. A convergence criterion based on the relative difference between the current and the previous iteration is used. When this difference reaches 10^{-5}, the solution is assumed to have converged and the iterative process is terminated.

The effect of the grid size $\Delta\eta$ and $\Delta\xi$ and the edge of the boundary layer η_∞ on the solutions is also examined. The results presented here are independent of the grid size and η_∞ at least up to the 3rd decimal place. Here we have taken $\Delta\eta = 0.05$, $\Delta\xi = 0.02$ and $\eta_\infty = 10$.

4. Results and discussion

In order to assess the accuracy of our method, we have compared the surface skin friction coefficient $(Re_x^{1/2}C_{fx})$ and the Nusselt number $(Re_x^{-1/2}Nu_x)$ for the VWT case when $\epsilon_1 = \epsilon_2 = m = 0$ with those of Chen and Mucoglu [1]. The corresponding results for the VHF case have been compared with those of Mucoglu and Chen [2]. In both the cases, the results are found to be in very good agreement. The comparison is presented in Tables 1 and 2.

It may be noted that for computation, we have taken to slots in the intervals $[0.5, 0.8]$ and $[1.2, 1.5]$. The wall is cooled or heated in these intervals and in the remaining portion the wall is at a constant temperature T_0 $(> T_\infty)$. Also injection or suction is applied only in these slots. In the remaining portion of the wall, the wall is non-permeable. Similarly, the heat flux is imposed only in these slots. We have taken $Re_R = 10^3$.

Figs. 2 and 3 show the effect of wall cooling $(\epsilon_2 < 0)$ and wall heating $(\epsilon_2 > 0)$ on the skin friction coefficient $(Re_x^{1/2}C_{fx})$ and the Nusselt number $(Re_x^{-1/2}Nu_x)$ for the VWT case when $\lambda = 0$ and 1, $\epsilon_1 = 0$, $0 \leqslant \xi \leqslant 2$, $Pr = 0.7$. The results for $\epsilon_2 = 0$ (without heating or cooling) are also shown. The effect of wall cooling/heating in the two slots is found to be more pronounced on the Nusselt number than on the skin friction, because wall cooling/heating directly affects the thermal field, where as its effect on the velocity field is indirect. In the region beyond the slots, the Nusselt number for the wall cooling $(\epsilon_2 < 0)$ is more than that of the wall heating. This behaviour is due to the fact that for the wall cooling the temperature difference between the wall and the fluid near the wall increases. Consequently, the temperature gradient and hence the heat transfer (Nusselt number) increase. The effect of wall heating is opposite to that of the wall cooling, but it is not a mirror reflection of the wall cooling. Since the positive buoyancy force $(\lambda > 0)$, which assist the flow, acts like a favourable pressure gradient, the fluid in the boundary layer gets accelerated. This in turn reduces the momentum and thermal boundary layer thicknesses. Consequently, both the velocity and temperature gradients and hence the skin friction and the Nusselt number increase with λ. Since the buoyancy parameter λ is multiplied by ξ (see Eq. (6)),

Table 1
Comparison of skin friction and heat transfer results $(Re_x^{1/2}C_{fx}, Re_x^{-1/2}Nu_x)$ for VWT case when $\epsilon_1 = \epsilon_2 = m = 0$, $Pr = 0.7$

ξ	Ω	Present results		Chen and Mucoglu [1]	
		$Re_x^{1/2}C_{fx}$	$Re_x^{-1/2}Nu_x$	$Re_x^{1/2}C_{fx}$	$Re_x^{-1/2}Nu_x$
0	0	1.3281	0.5854	1.3282	0.5854
0	1	4.9663	0.8219	4.9668	0.8221
0	2	7.7119	0.9302	7.7126	0.9305
1	0	1.9167	0.8666	1.9172	0.8669
1	1	5.2578	1.0617	5.2584	1.0621
1	2	7.8863	1.1685	7.8871	1.1690
2	0	2.3975	1.0963	2.3981	1.0968
2	1	5.6993	1.2712	5.7001	1.2718
2	2	8.3555	1.3741	8.3566	1.3747

Table 2
Comparison of skin friction $(Re_x^{1/2}C_{fx})$ and reciprocal of heat transfer $(Re_x^{1/2}(Nu_x)^{-1})$ for VHF case when $\epsilon_1 = \epsilon_3 = m = 0$, $Pr = 0.7$

ξ	Ω^*	Present results		Chen and Mucoglu [2]	
		$Re_x^{1/2}C_{fx}$	$Re_x^{1/2}(Nu_x)^{-1}$	$Re_x^{1/2}C_{fx}$	$Re_x^{1/2}(Nu_x)^{-1}$
0	0	1.3281	2.4636	1.3282	2.4637
0	1.0	6.3659	1.7922	6.3665	1.7923
0	1.5	8.0157	1.6908	8.0165	1.6911
1	0	1.9108	1.8539	1.9113	1.8543
1	1.0	5.9407	1.4701	5.9414	1.4705
1	1.5	7.3443	1.3965	7.3451	1.3970
2	0	2.3840	1.5337	2.3847	1.5343
2	1.0	5.9312	1.3001	5.9322	1.3007
2	1.5	7.2546	1.2450	7.2558	1.2458

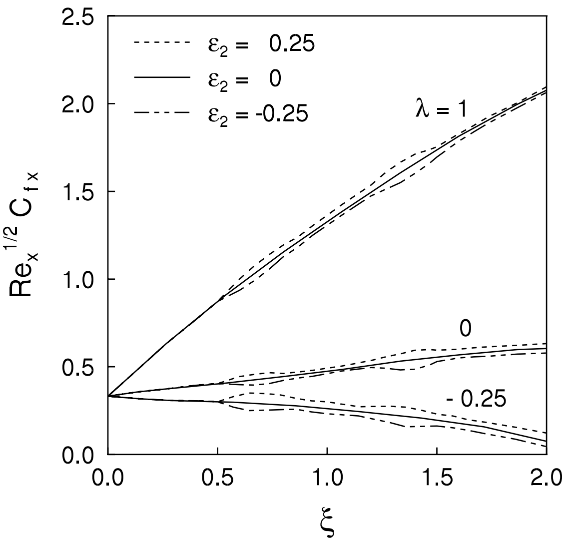

Fig. 2. Effect of wall cooling/heating on the skin friction coefficient $Re_x^{1/2}C_{fx}$ for $\lambda = -0.25$, 0 and 1, $\epsilon_1 = 0$, $Pr = 0.7$ (VWT case).

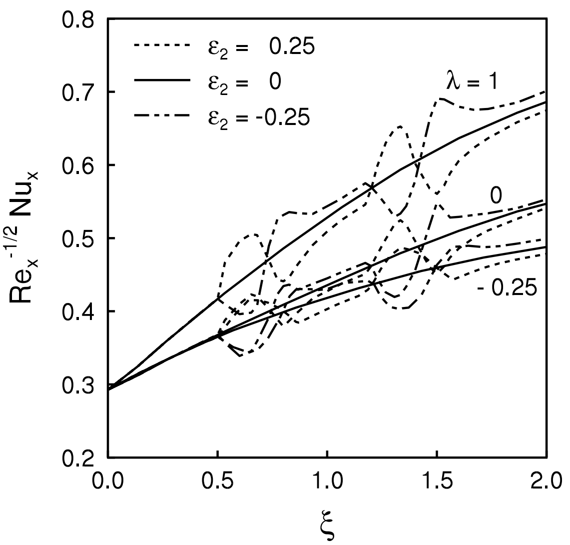

Fig. 3. Effect of wall cooling/heating on the Nusselt number $Re_x^{-1/2}Nu_x$ for $\lambda = -0.25$, 0 and 1, $\epsilon_1 = 0$, $Pr = 0.7$ (VWT case).

the effect of the buoyancy parameter vanishes at $\xi = 0$, but increases with ξ. For a fixed λ, both the skin friction and the Nusselt number increase with ξ, because the velocity and temperature gradients at and near the wall increase with ξ. It may be noted that the thermal boundary layer is thicker than the momentum boundary layer. Since the negative buoyancy parameter ($\lambda < 0$) acts like an adverse pressure gradient, the momentum and thermal boundary layers grow. Consequently, the skin friction and heat transfer are reduced. Further for $\lambda < 0$, the skin friction decreases with increasing ξ, but the heat transfer increases.

Figs. 4 and 5 present the effect of injection ($\epsilon_1 > 0$), suction ($\epsilon_1 < 0$) and without cooling/heating ($\epsilon_2 = 0$) on the skin friction coefficient ($Re_x^{1/2}C_{fx}$) and the Nusselt number ($Re_x^{-1/2}Nu_x$) for the VWT case when $\lambda = 1$, $Pr = 0.7$, $\epsilon_2 = 0$, $0 \leqslant \xi \leqslant 2$. Both the skin friction and the Nusselt number decrease due to injection, but they in-

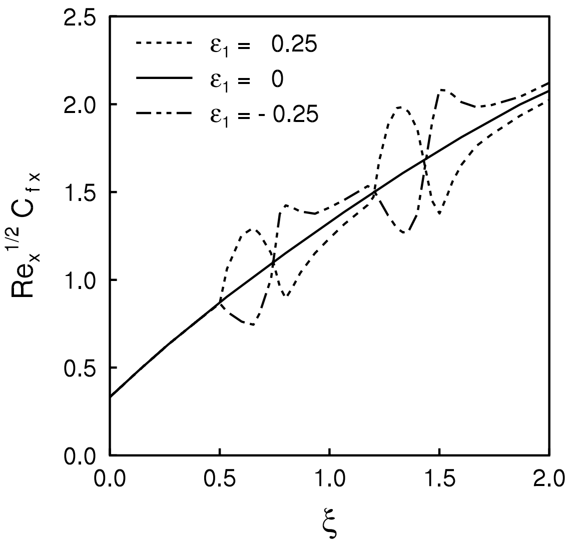

Fig. 4. Effect of injection/suction on the skin friction coefficient $Re_x^{1/2}C_{fx}$ for $\lambda = 1$, $\epsilon_2 = 0$, $Pr = 0.7$ (VWT case).

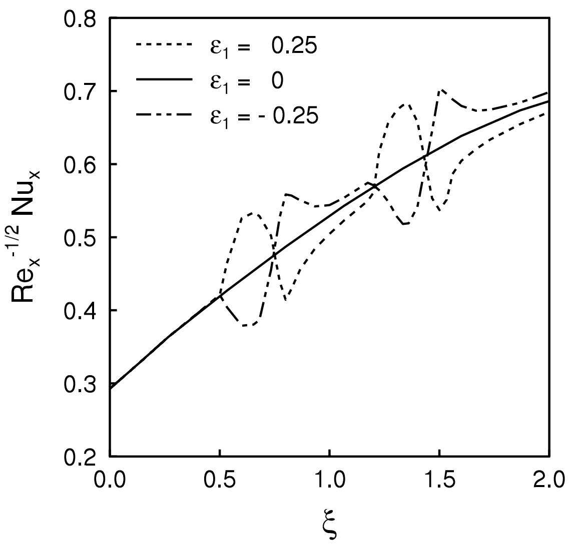

Fig. 5. Effect of injection/suction on the Nusselt number $Re_x^{-1/2}Nu_x$ for $\lambda = 1$, $\epsilon_2 = 0$, $Pr = 0.7$ (VWT case).

crease due to suction. This trend is due to the growth in the momentum and thermal boundary layers caused by injection. The effect of suction is opposite to that of injection, but it is not the mirror reflection of each other.

Figs. 6–8 give the corresponding results for the Nusselt number and the skin friction coefficient for the variable/constant heat flux case (VHF/CHF case). The results are found to be qualitatively similar to those

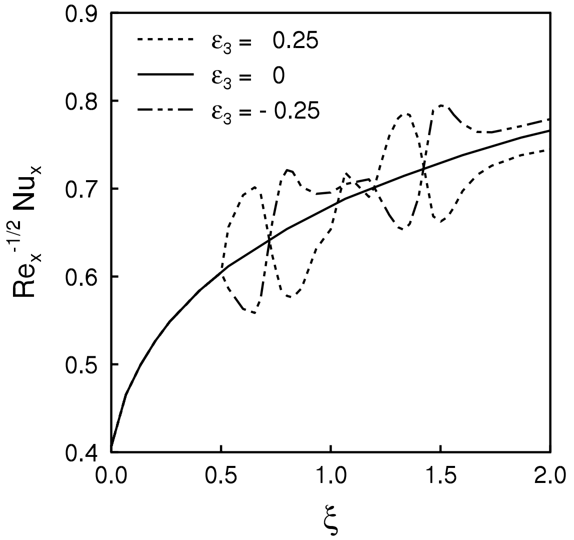

Fig. 6. Effect of reduction/increase of wall heat flux on the Nusselt number $Re_x^{-1/2}Nu_x$ for $\lambda^* = 1$, $\epsilon_1 = 0$, $Pr = 0.7$ (VHF case).

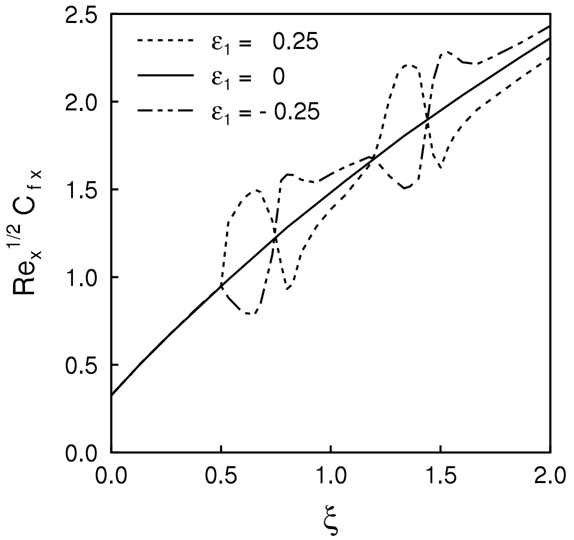

Fig. 7. Effect of injection/suction on the skin friction coefficient $Re_x^{1/2}C_{fx}$ for $\lambda^* = 1$, $\epsilon_3 = 0$, $Pr = 0.7$ (CHF case).

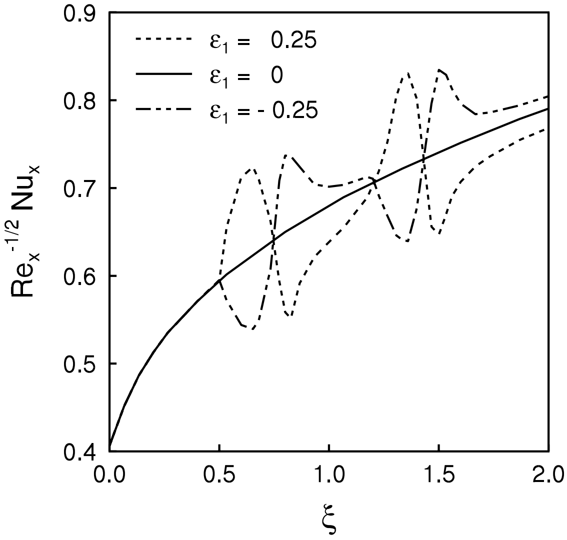

Fig. 8. Effect of injection/suction on the Nusselt number $Re_x^{-1/2}Nu_x$ for $\lambda^* = 1$, $\epsilon_3 = 0$, $Pr = 0.7$ (CHF case).

of the VWT/CWT case. Hence they are not discussed here. The Nusselt number and the skin friction coefficient for the VHF/CHF case are more than those of the VWT/CWT case.

5. Conclusions

The effect of the localized cooling/heating is found to be more pronounced on the Nusselt number than on the skin friction coefficient. Also the effect of the localized heating and suction is not a mirror reflection of cooling and injection, respectively. The Nusselt number and skin friction coefficient increase with the positive buoyancy force and suction, but they reduce due to injection. The skin friction and the Nusselt number for the variable/constant heat flux case are more than those of the variable/constant wall temperature case.

References

[1] T.S. Chen, A. Mucoglu, Buoyancy effects on forced convection along a vertical cylinder, J. Heat Transfer 97 (1975) 198–203.

[2] A. Mucoglu, T.S. Chen, Buoyancy effects on forced convection along a vertical cylinder with uniform surface heat flux, J. Heat Transfer 98 (1976) 523–525.

[3] E.M. Sparrow, H. Quack, C.J. Boerner, Local nonsimilarity boundary layer solutions, AIAA J. 8 (1970) 1936–1942.

[4] E.M. Sparrow, H.S. Yu, Local nonsimilarity thermal boundary solutions, J. Heat Transfer 93 (1971) 328–334.

[5] M.N. Bu, T. Cebeci, Combined free and forced convection in vertical slender cylinders, J. Heat Transfer 107 (1986) 476–478.
[6] T.Y. Wang, C. Kleinstrever, General analysis of steady laminar mixed convection heat transfer on vertical slender cylinders, J. Heat Transfer 111 (1989) 393–398.
[7] H.B. Keller, T. Cebeci, Accurate numerical methods for boundary layer flows: II. Two-dimensional turbulent flows, AIAA J. 10 (1972) 1193–1199.
[8] S.L. Lee, T.S. Chen, B.F. Armaly, Mixed convection along vertical cylinders and needles, in: Proc. 8th Int. Heat Transfer Conf., vol. 3, 1986, pp. 1425–1432.
[9] S.L. Lee, T.S. Chen, B.F. Armaly, Mixed convection along vertical cylinders and needles with uniform surface heat flux, J. Heat Transfer 109 (1987) 711–716.
[10] S.L. Lee, T.S. Chen, B.F. Armaly, New finite difference solution methods for wave instability problems, Numer. Heat Transfer 10 (1986) 1–18.
[11] R.L. Burden, J.D. Faires, Numerical Analysis, 3rd ed., Prindle, Weber and Schmitt Publishers, Boston, MA, 1985, pp. 117–129.
[12] T.Y. Na, I. Pop, Flow and heat transfer over a longitudinal circular cylinder moving in a parallel or reversely to a free stream, Acta Mech. 118 (1996) 185–195.
[13] H.S. Takhar, A.J. Chamkha, G. Nath, Combined heat and mass transfer along a vertical moving cylinder with a free stream, Heat Mass Transfer 36 (2000) 89–96.
[14] F.G. Blottner, Finite difference methods of solution of the boundary layer equations, AIAA J. 8 (1970) 193–205.